

## Supporting Information

### **Interfacing Droplet Microfluidics with Antibody Barcodes for Multiplexed Single-Cell Protein Secretion Profiling**

Tahereh Khajvand,<sup>a</sup> Peifeng Huang,<sup>a</sup> Linmei Li,<sup>b</sup> Mingxia Zhang,<sup>a</sup> Fengjiao Zhu,<sup>b</sup> Xing Xu,<sup>a</sup> Mengjiao Huang,<sup>a</sup> Chaoyong Yang,<sup>a,c</sup> Yao Lu,<sup>b\*</sup> Zhi Zhu,<sup>a\*</sup>

#### **Table of Contents**

|  |   |
|--|---|
| Experimental Procedures.....   | 2 |
| Design and Fabrication of Integrated Single-Cell Secretome Barcode Microchip ..... | 2 |
| Fabrication of the Two-Layered PDMS Capture Microchip .....                        | 2 |
| Fabrication of High-Density Antibody Barcode Microarrays .....                     | 4 |
| Cell Culture and Patient Tissue Samples.....                                       | 4 |
| MicroELISA Procedures.....   | 5 |
| Data and Statistical Analyses .....  | 5 |
| Results and Discussion.....  | 5 |
| References .....   | 8 |

## Experimental Procedures

### Design and Fabrication of Integrated Single-Cell Secretome Barcode Microchip

This integrated microfluidic chip is comprised of three PDMS substrates as shown in **Figure S1A**:  $\mathcal{E}$  PDMS microvalve slab as a control layer;  $\&$  PDMS chamber array as a flow layer;  $\bullet$  PDMS barcode chip for flow-based antibody patterning. The PDMS microvalve layer with PDMS chamber array forms the microchip for capture, isolation, and incubation of individual cells. Microfluidic capture chips are designed with 1-row of 100-picochambers allowing studies of a maximum of 100 single-cells. The antibody barcode array slide with the capture chip form an integrated barcode chip for single-cell secretome analysis. The antibody barcode array slide comprises long serpentine channel barcodes, each of which contains up to 5 stripes of different antibodies, immobilized on a poly-L-lysine (PLL) glass slide. To capture/isolate single-cells and confine the secretion proteins in the detection area, two sets of horizontal microvalves in one layer are embedded, in which the first one is close to the capture channel (V1) and the second one is close to the buffer channel (V2). By hydraulic pressurization of the valves, the membrane is deflected down into the capture channels, causing it to seal against the glass substrate. The actuation pressure of the control layer mainly depends on the valve dimensions and membrane thickness. Microvalves isolate the chip into 100-picochambers for downstream cell capture, incubation, and protein assays.

The most successful patterning technique in microfabrication is photolithography to transfer microscale patterns to photosensitive materials by selective exposure to optical radiation.<sup>1</sup> Briefly, after mask design using computer-aided design (AutoCAD2016) software, three masters are fabricated from a SU-8 (Microchem Corp)-coated silicon wafer (Compart Technology Ltd.) to yield features in  $\mu\text{m}$ . Photoresist-coated silicon wafers are exposed through the photomask. Exposure causes a mask aligner to pass a controlled amount of ultraviolet light through the mask onto the coated wafer, and the photomask design is transferred to the silicon surface. Developer solution removes residual resist and leaves behind a negative 3D image of the final pattern. The silicon then acts as a master mold for casting replicas of transparent PDMS polymer by soft lithography.<sup>2</sup>

### Fabrication of the Two-Layered PDMS Capture Microchip

Using standard photolithography techniques, two relief molds with different patterns  $\mathcal{E}$  &  $\&$  are created, each comprising a pattern of negative photoresist on a silicon wafer. One mold represents a pattern of fluid channels and creates the “fluid layer (capture layer)”; the other represents control channels and creates the “control layer (microvalves)” composed of microchannels that act as hydraulic lines for applying negative pressure. In this device, a push-down configuration is utilized with a thick control layer bonded to a thin flow layer underneath. The molds for the capture layer and valve layer are fabricated with SU-8 2015 negative photoresist (spin cycle: 1800 rpm; 200 rpm/s, 46 s; height  $\sim 20 \mu\text{m}$ ) and SU-8 3050 negative photoresist (spin cycle: 3500 rpm; 200 rpm/s, 46 s; height  $\sim 35 \mu\text{m}$ ), pre-baked at 65°C and 95°C for 15 min, 65°C and 95°C for 10 min, followed by UV exposure at a dose of 150 mJ/cm<sup>2</sup> and 75 mJ/cm<sup>2</sup>, respectively. This was followed by post-baking at the same heating temperatures and times as the pre-baking, and development and rinsing in propylene-glycol-monomethyl-ether-acetate (PGMEA) and isopropyl alcohol. In the optimized conditions, the thick control layer (valve layer) is molded with 10:1(w/w) mixture of GE RTV 615 PDMS prepolymer part A: part B, and the flow layer (capture layer) is formed by spin-coating a 23:1(w/w) mixture of Sylgard 184 (Dow Corning) PDMS part A:part B on the flow layer mold at 2400 rpm for 60 s. Microvalve and capture layers are cured at 75°C, for 11 min and 53°C for 4.5 min, respectively, during which the control layer is cut from its mold and aligned to the flow layer. An additional 30 min of thermal treatment at 60°C ensures that the two layers bond into a monolithic device, which is then peeled from its mold and drilled to create appropriate access holes. During this time, excess functional groups in the two layers interact to form covalent bonds across the interface. Finally, the two-layer chip is sealed to the micropattern glass slide to form an integrated barcode chip. An assembly of a complete single-cell secretome analysis device is shown in **Figures S1B and S1C**. It is noted that when the thick layer is released from the mold, it shrinks by 0.5–2.5% in each dimension, depending on curing temperature,

PDMS component ratios, and layer thickness. So, to achieve the highest success rate in fabricating the capture chip and precise control of fluid flow within microfluidic channels, the most important factors in chip fabrication were optimized as indicated in **Table S1**.

**Figure S2B**. represents the 3D topography and optical microscopy image of two layers of microchip after the molding process. The process of making the master by changing the parameters such as spinning speed and exposure time was optimized. The results indicate that cell capture channel and microvalve channels have intact shape, and that the parameters of each part of the channels meet the design criteria. Therefore, the templates can be used for the production of PDMS chips. The valve channel width and the distance between the two valve channels are 25  $\mu\text{m}$  and 150  $\mu\text{m}$ , respectively. Spin-coating is utilized to create a thin uniform film of the capture layer, whereby the thickness of the film can be precisely controlled. The capture layer height and valve channel height are 20  $\mu\text{m}$  and 35  $\mu\text{m}$ , respectively, which show clear outlines. The uniformity feature of the capture array was investigated, and a statistical chart of the average height of four capture layers is shown in **Figure S2C**. The average height is  $\sim 20 \mu\text{m}$  with a standard deviation of 0.56  $\mu\text{m}$ , indicating good uniformity, which allows cells to pass smoothly and ensures that the pneumatically actuated microvalves provide uniform isolation during microchip operation.

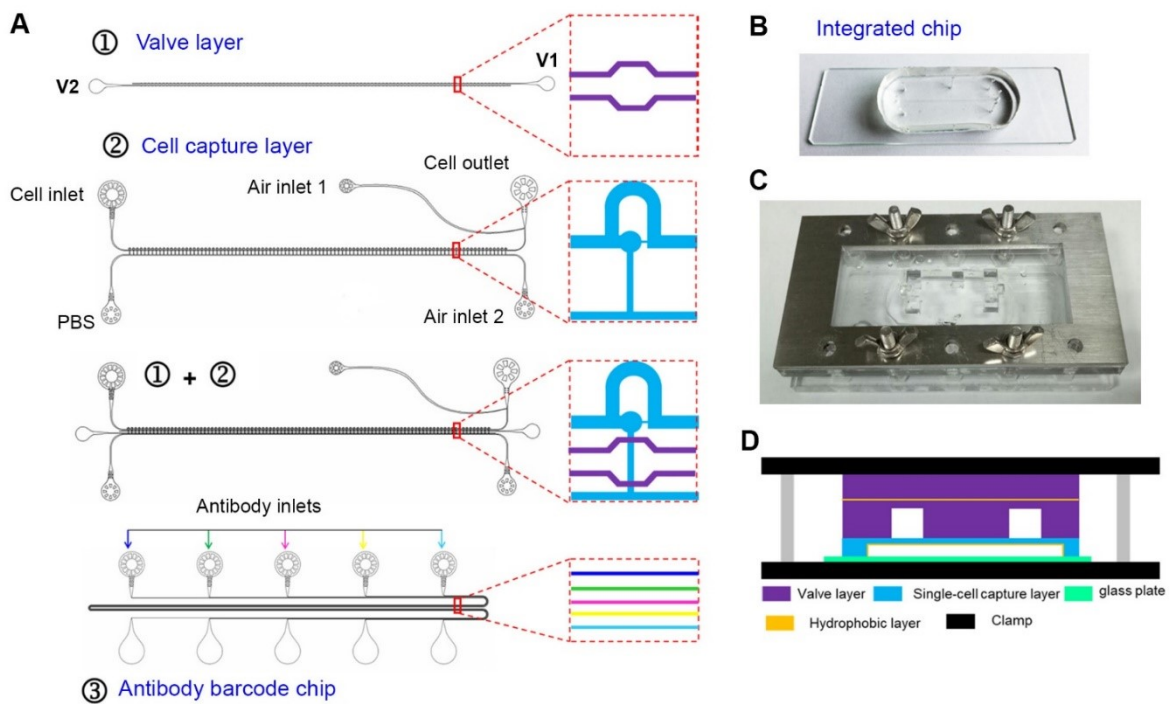


**Figure S1.** (A) CAD design of integrated single-cell secretome analysis device including a high-density antibody array glass slide clamped together with a 100-chamber PDMS slab, and a PDMS barcode chip for flow-based antibody patterning. (B) Photograph of actual integrated chip. (C) Representative image of single-cell analysis assembled device. The complete single-cell secretome analysis device consists of a high-density antibody array glass slide and a 100- picochamber PDMS slab that were clamped together with a metal holder and two transparent plates using springs and screws. (D) Schematic assembly of a complete integrated single-cell secretome analysis device modified with a hydrophobic barrier (EGC-1720).

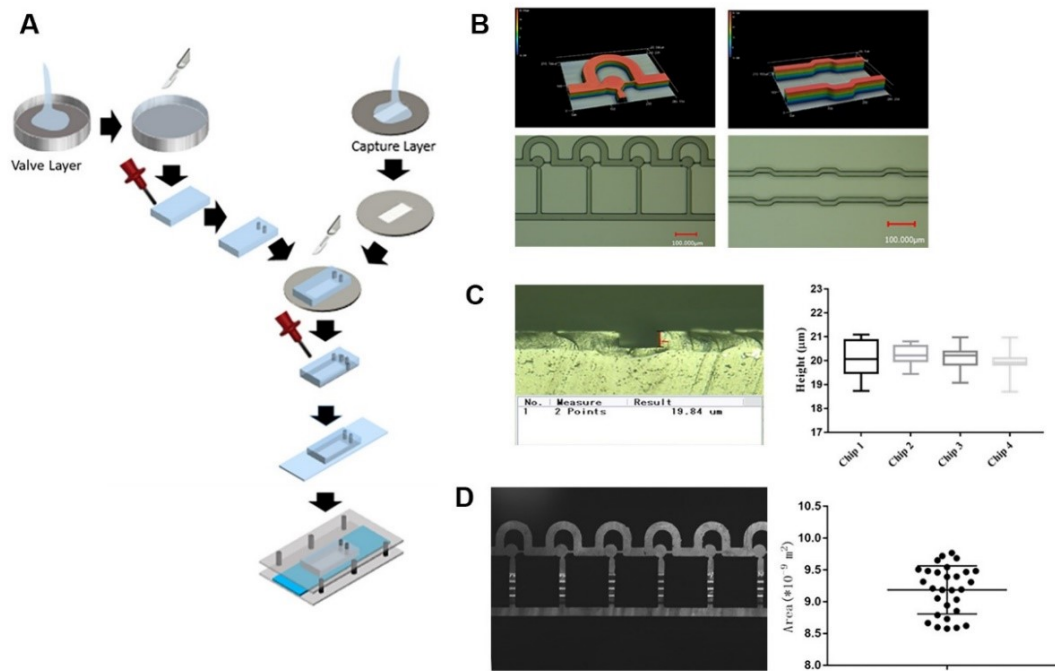


**Figure S2.** Fabrication procedure and characterization of the integrated barcode microchip. **(A)** 2-layer push-down microfluidic devices fabricated by multi-layer soft lithography. **(B)** The 3D topography of SU8 silicon models of cell capture channel and microvalve channels by 3D laser scanning confocal microscopy. **(C)** Single-cell capture layer height and uniformity. Cross-section of capture layer and height uniformity of chambers. **(D)** Alignment of microvalve layer in integrated microchips and uniformity test of incubated solution area in capture chip.

### Fabrication of High-Density Antibody Barcode Microarrays

The procedure for flow patterning of the antibody barcode microarray is performed as previously described.<sup>3</sup> Briefly, the PDMS microfluidic chip containing parallel microfluidic channels for flow-patterning antibody barcode array is constructed using standard soft lithographic techniques (● **Figure S1A**). RTV615 (MOMENTIVE) mixed in a 10:1 (w/w) ratio of resin to cross-linker is poured over the mold. After degassing, the device is cured for 30 min at 75°C and peeled off the master. Access holes for fluidic tubing are created using a biopsy punch to allow fluids to flow into the channels. The PDMS microchip is attached to the PLL glass to form long and narrow microchannels for flow patterning. Finally, it is baked for 2 h at 80°C to strengthen the bond between the PDMS mold and the glass slide. This chip comprises inlets leading to one repeat of individual long microchannels, each of which can contain one stripe of distinctive antibodies immobilized on a modified surface (PLL glass slide). For the flow patterning of the antibody barcodes, 1.5 µL of each antibody (**Table S2**) was injected into microchannel inlets separately and flowed until completely dry with 1-psi pressured N<sub>2</sub>. After flow patterning, PDMS slab was released and the glass slide was blocked with 1% bovine serum albumin (BSA) for 1 h at room temperature to reduce nonspecific adsorption. Then, the glass slide was rinsed with 1× PBS and deionized (DI) water for desalination and gently blown dry with forced N<sub>2</sub>. Functionalized barcode slides were spun dry in a slide centrifuge and stored at 4 °C before use.

### Cell Culture and Patient Tissue Samples

Human glioblastoma multiforme cell line U87 (American Type Culture Collection, ATCC) was cultured in medium RPMI 1640 (Gibco, Invitrogen) with 10% fetal bovine serum (FBS, ATCC) and 1% antibiotics (100 U/mL of penicillin G sodium, 100 U/mL of streptomycin). Before being loaded into the microdevice, the cells were trypsinized with 0.25% trypsin/0.02% EDTA for 3 min, centrifuged at 1000 rpm for 5 min, and resuspended in fresh medium with concentration of 5×10<sup>6</sup> cells/mL.

Human U937 cell line was cultured in RPMI 1640 medium (Gibco, Invitrogen) supplemented with 10% FBS, ATCC at 37°C and 5% CO<sub>2</sub>. Every 100 µL of U937 cell suspension was differentiated into macrophages by treating with 1 µL 50 ng/mL phorbol 12-myristate 13-acetate (PMA, Fisher) for 48 h, followed by culture in fresh standard medium for 24 h. The cells were challenged by 1 µL 100 ng/mL lipopolysaccharide (LPS, Calbiochem) to activate Toll-like receptor 4 (TLR4) signaling before the suspension was loaded into the capture chip.

Human oral squamous carcinoma cell line (SCC6) (American Type Culture Collection) was cultured in MEM medium (Gibco; Thermo Fisher Scientific) with 10% FBS (Gibco; Invitrogen), 1% antibiotics (100 U/mL of penicillin G sodium, 100 U/mL of streptomycin) and 1% MEM Non-Essential Amino Acid (Life Technologies). The cells were detached with 0.25% trypsin/0.02% EDTA for 4 min, centrifuged at 300 rpm for 5 min, washed, and resuspended in fresh medium before use.

Human SCC patient samples were obtained from the Affiliated Hospital of Dalian Medical University. The collection and use of human samples were approved by the Ethics Committee of Dalian Medical University (Ethics Reference NO: YJ-KY-FB-2016-45).

### **MicroELISA Procedures**

After the microchip incubation for 4 h at 37 °C, 5% CO<sub>2</sub> incubators, protein secretions were analyzed via microELISA assay. First, the flow patterned antibody glass slide was disassembled carefully and blocked with 3% BSA for 30 min. Then, a cocktail solution of biotin-labeled detection antibodies (**Table S2**) was pipeted onto the glass slide and incubated for 45 min at room temperature to complete the immunoreaction followed by washing with 1% BSA solution. Next, the streptavidin-labeled APC (eBioscience, 1:200 dilutions in 1% BSA solution) was added and glass slide soaked for another 20 min. Following, the glass slide was washed again and blocked with 3% BSA for 20 min. After that, the glass slide was rinsed in PBS, PBS, DI water, DI water sequentially and blown dry. Finally, the glass slide was scanned and fluorescence result analyzed by the GenePix 4300A scanner and software (Molecular Devices, USA).

### **Data and Statistical Analyses**

Microarray slides were scanned using a GenePix 4300 (Axon Instruments) scanner to acquire the microarray images, which were subsequently processed with GenePix Pro software (Molecular Devices) to generate the expression data in GPR (Genepix Result File) format using the median fluorescent intensity of a feature spot on a microarray slide. The averaged fluorescence intensities for all barcodes were obtained by custom-developed GraphPad Prism and Excel Microsoft. Heat maps were generated with software Cluster/Treeview (Eisen Laboratory). Statistical analysis was conducted in Excel, GraphPad Prism, and Python script.

## Results and Discussion

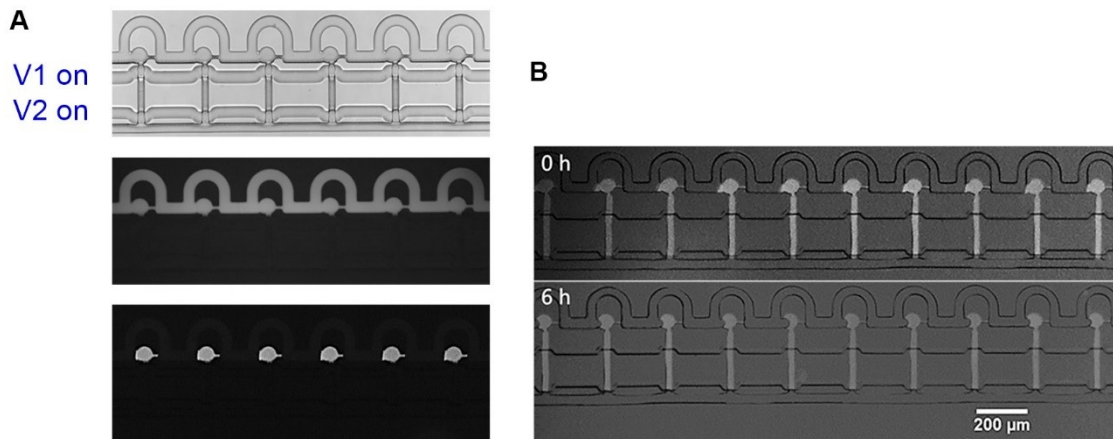


**Figure S3.** (A) Representative images verifying the excellent isolation effect of the blocking valves and droplet generation to separate picochamber units. (B) Long-term droplet storage characterization. Photographs of a stored droplet in a modified PDMS chip taken at  $t = 0$  and  $t = 6$  h, respectively; Photos show that microchip modification significantly improved the channels' storage properties.

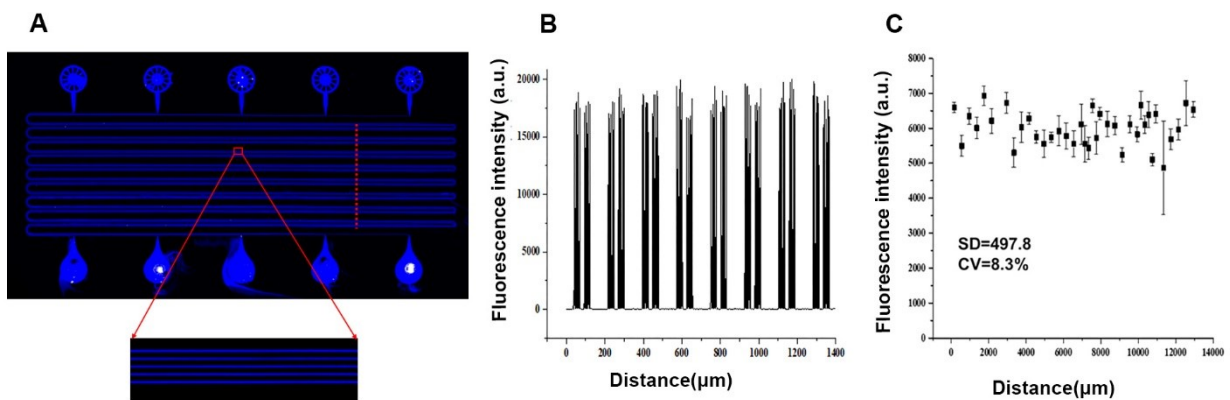


**Figure S4.** Evaluation of the protein coating uniformity flow-patterned with antibody barcode microchannel. (A) Flow-patterning guided fabrication of high-density barcode antibody microarray; whole glass slide fluorescence scanning; (B), and (C) quantification of fluorescence intensity across the flow-patterned PLL slide, revealing excellent uniformity of the immobilized proteins (FITC-BSA 5 mg/mL, 2  $\mu\text{L}$ ), which ensures the validity of using this high-density barcode array technology to assess single-cell heterogeneity.

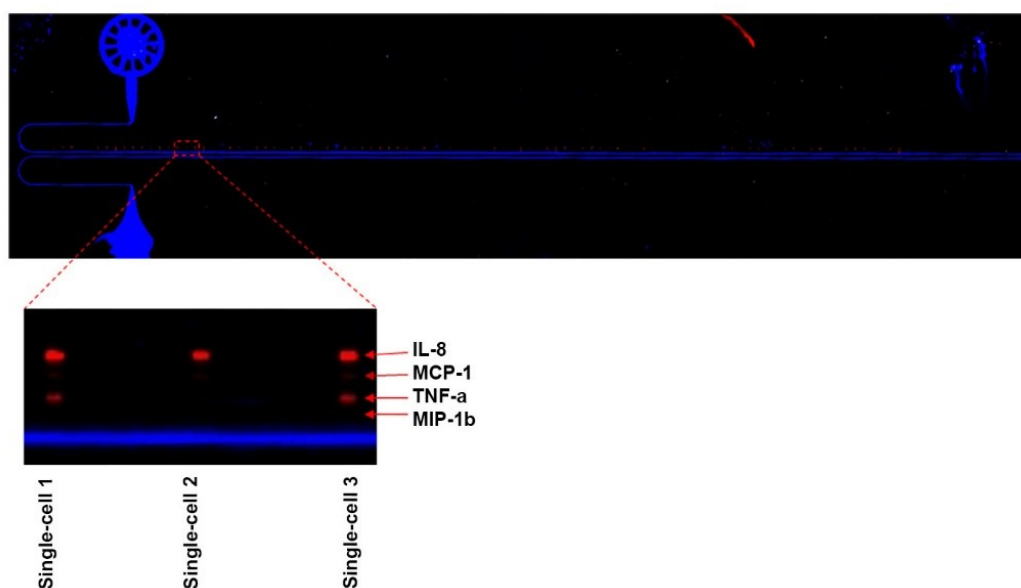


**Figure S5.** Fluorescent readout map and partial enlargement of secreted protein by macrophage single-cells without LPS stimulation (incubation time: 4 h). The glass slide microarray was scanned using a high-resolution fluorescence scanner (Axon GenePix 4300). Two-color lines were created with immobilized FITC-BSA (488, blue) and streptavidin-APC (Cy5, 650, red) for specific protein detection within each detection area.

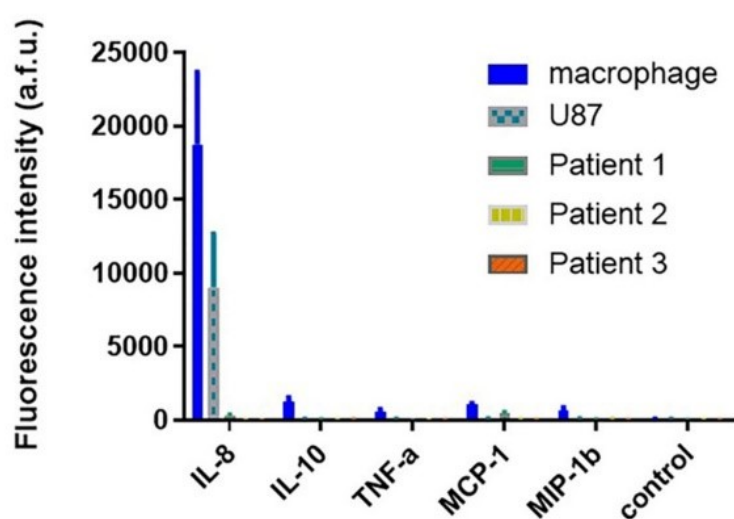


**Figure S6.** Population level protein secretion profile. Proteins secreted were measured from a large population of macrophage, U87, and three patients by a conventional antibody microarray.

**Table S1.** Optimized values of 2-layer microfluidic devices through multi-layer soft lithography.

| Microvalve layer             |                    | Capture layer               |                    |                    | Two-layer chip                    |   |             |
|------------------------------|--------------------|-----------------------------|--------------------|--------------------|-----------------------------------|---|-------------|
| Base/Curing agent by weight) | Curing temp & time | Base/Curing agent by weight | Curing temp & time | Spin coating (rpm) | Thermal bonding of the two layers | Thermal bonding of the glass slide to the PDMS chip | Performance |
| RTV 615 (10:1)               | 75°C; 11 min       | Sylgard 184 (23:1)          | 53°C; 4.5 min      | 2400, 1 min        | 60 °C; 30 min                     | 80 °C; 2 h  | Ⓡ           |

**Table S2.** Summary of antibodies (name, clone, company, catalog) used in this study (most are monoclonal antibodies).

| Protein | Capture antibody<br>Isotype/clone/vendor/catalog | Detection antibody<br>Isotype/clone/vendor/catalog |
|---------|--|--|
| TNF-a   | Mouse IgG1, κ /Mab11/Biolegend /502902           | Mouse IgG1, κ /MAB1/Biolegend/502802               |
| MIP-1b  | Mouse IgG1 kappa/A174E18A7/Invitrogen/AHC6114    | Mouse IgG2B /24006/RD/MAB271                       |
| MCP-1   | Mouse IgG1, κ /5D3-F7/Biolegend/502607           | Armenian Hamster IgG /2H5/Biolegend/505902         |
| IL-8    | Mouse IgG1, κ /H8A5/Biolegend/511502             | Mouse IgG1, κ /E8N1/Biolegend/511402               |
| IL-10   | Rat IgG2a, κ /JES3-12G8/Biolegend/501504         | Rat IgG1, κ /JES3-9D7/Biolegend/ 501402            |

**Table S3.** List of all proteins (full name and their functions in human physiology) incorporated in the microchip assay platform.

| Secreted Proteins | Full name                          | Function  |
|-------------------|------------------------------------|---|
| TNF-a             | Tumor necrosis factor alpha        | Acute phase reaction  |
| MIP-1b            | Macrophage inflammatory protein-1β | Chemoattractant for a variety of immune cells                                       |
| MCP-1             | Monocyte chemoattractant protein 1 | Recruit monocytes, memory T cells, and dendritic cells to the sites of inflammation |
| IL-8              | Interleukin 8                      | Chemotaxis  |
| IL-10             | Interleukin 10                     | Inhibit the synthesis of pro-inflammatory cytokine                                  |

## References



- 1 S. R. Quake, A. Scherer, *Science*, 2000, **290** (5496), 1536–1540.
- 2 G. Thuillier, C. K. Malek, *Microsyst. Technol.*, 2005, **12**, 180-185.
- 3 C. Ma, A. F. Cheung, T. Chodon, R. C. Koya, Z. Wu, C. Ng, E. Avramis, A. J. Cochran, O. N. Witte, D. Baltimore, B. Chmielowski, J.S. Economou, B. Comin-Anduix, A. Ribas, J. R. Heath, *Cancer Discov.*, 2013, **3** (4), 418–429.